2004

Field-induced domain interpenetration in tetragonal ferroelectric crystal

Xiaoli Tan
Iowa State University, xtan@iastate.edu

J. K. Shang
University of Illinois at Urbana-Champaign

Field-induced domain interpenetration in tetragonal ferroelectric crystal

Abstract
Ferroelectric domain structures of a 〈001〉 -oriented lead magnesium niobate–lead titanate tetragonal crystal were examined under cyclic bipolar electric fields. Complex patterns of orthogonal domain strips were found to emerge from a simple structure of parallel strips of 90°domains. Near the boundary between the two orthogonal sets of the domain strips, domains were forced to intersect, creating charged domain walls at the intersections. With continued electric cycling, direct impingement of individual domains resulted in domain interpenetration and fine domain cells in the boundary region. Away from the boundary region, initial domain walls were withdrawn and replaced by the walls along a different orientation, resulting in separate areas that each contained a single set of parallel strips of domains. A model based on 180° domain switching is suggested to explain interpenetration of the domains and the withdrawal of the original domain walls.

Keywords
Domain walls, Ferroelectric domain structure, Crystal structure, Electric fields, Magnesium, Titanates

Disciplines
Materials Science and Engineering

Comments
The following article appeared in *Journal of Applied Physics* 95 (2004): 635 and may be found at http://dx.doi.org/10.1063/1.1635970.

Field-induced domain interpenetration in tetragonal ferroelectric crystal

X. Tan and J. K. Shang

Citation: Journal of Applied Physics **95**, 635 (2004); doi: 10.1063/1.1635970
View online: http://dx.doi.org/10.1063/1.1635970
View Table of Contents: http://scitation.aip.org/content/aip/journal/jap/95/2?ver=pdfcov
Published by the AIP Publishing

Field-induced domain interpenetration in tetragonal ferroelectric crystal

X. Tan[a)]
Department of Materials Science and Engineering, Iowa State University, Ames, Iowa 50011

J. K. Shang
Department of Materials Science and Engineering, University of Illinois at Urbana–Champaign, Urbana, Illinois 61801

(Received 10 September 2003; accepted 30 October 2003)

Ferroelectric domain structures of a ⟨001⟩-oriented lead magnesium niobate–lead titanate tetragonal crystal were examined under cyclic bipolar electric fields. Complex patterns of orthogonal domain strips were found to emerge from a simple structure of parallel strips of 90° domains. Near the boundary between the two orthogonal sets of the domain strips, domains were forced to intersect, creating charged domain walls at the intersections. With continued electric cycling, direct impingement of individual domains resulted in domain interpenetration and fine domain cells in the boundary region. Away from the boundary region, initial domain walls were withdrawn and replaced by the walls along a different orientation, resulting in separate areas that each contained a single set of parallel strips of domains. A model based on 180° domain switching is suggested to explain interpenetration of the domains and the withdrawal of the original domain walls. © *2004 American Institute of Physics.* [DOI: 10.1063/1.1635970]

I. INTRODUCTION

Ferroelectric domains are the volumes in which there exist homogeneous electrical polarizations in ferroelectrics. As basic structural units, they play a key role in determining dielectric, piezoelectric, and ferroelectric properties of ferroelectrics. When a ferroelectric solid is subject to an external field, domains may respond to the applied field by expansion of the domains with favorable polarization directions at the expense of those with unfavorable orientations through domain wall movement. The wall movement can contribute 40% to the dielectric constant in barium titanate ceramics.[1] In $Pb(Mg_{1/3}Nb_{2/3})O_3–PbTiO_3$(PMN–PT) and $Pb(Zn_{1/3}Nb_{2/3})O_3–PbTiO_3$ (PZN–PT) single crystals, ultrahigh piezoelectric properties were only found in multiple-domain states resulting from ⟨001⟩ poling.[2–4]

The polarization switching can cause a transformation of the domain structure, leading to formation of complex domain patterns. The complex domain structures often consist of zones with parallel domain strips. When those domains approach each other, domain intersections may develop.[5–9] As a result of the domain intersection, electric as well as mechanical complications may arise in the ferroelectric response of a multidomained structure. To the electric behavior, the domain intersection carries excess electrical charges, and thus provide a convenient path for charge injection, which in turn may cause electric fatigue.[7] To the mechanical response, the intersection produces local lattice distortion, which may result in changes in domain wall density[8] or local fracture.[10,11]

The domain intersections have been observed in as-grown single crystals,[11–13] domain-engineered crystals,[14,15] electric field cycled crystals,[7,16] and polycrystalline ceramics.[5,8,9] However, domain structures emerging from the intersection are yet to be understood. In this study, domain intersections were produced in a tetragonal ferroelectric crystal by cyclic bipolar electric fields. The crystal orientation and field direction were selected so that the focus could be made on intersections of those with in-plane polarizations only. Under these conditions, one set of 90° domains was found to penetrate into another set and eventually replace the other set of domains. Crystallographic analysis indicated that 180° domain switching at the intersection could result in the observed evolution of the domain structure.

II. EXPERIMENTAL PROCEDURE

A single crystal of 0.65PMN–0.35PT was grown with the vertical Bridgman method, using a sealed platinum crucible by (110) seeding. Specimens for optical microscopy study of $6.0\times3.0\times0.8\ mm^3$ with surfaces parallel to pseudocubic {010} planes were cut from the crystal according to predetermined orientations by x-ray Laue diffraction. Two major surfaces of the specimens ($6.0\times3.0\ mm^2$) were polished with diamond paste down to near-mirror finish. In order to remove residual stress caused by sample preparation, polished specimens were annealed at 300 °C for 3 h.

The specimens were then electroded by evaporating Au to the two side surfaces of $6.0\times0.8\ mm^2$. The Au film electrodes were then connected to a high voltage (HV) power supply comprised of a Tektronix CFG 253 function generator and a Trek 610D HV amplifier. Cyclic sinusoidal electric fields of 30 Hz were applied across the specimens along the ⟨100⟩ direction to trigger the domain switching. Domain morphologies were examined with optical microscopy under cross-polarized light, and the images were recorded with an attached charge-coupled-device camera.

a)Electronic mail: xtan@iastate.edu

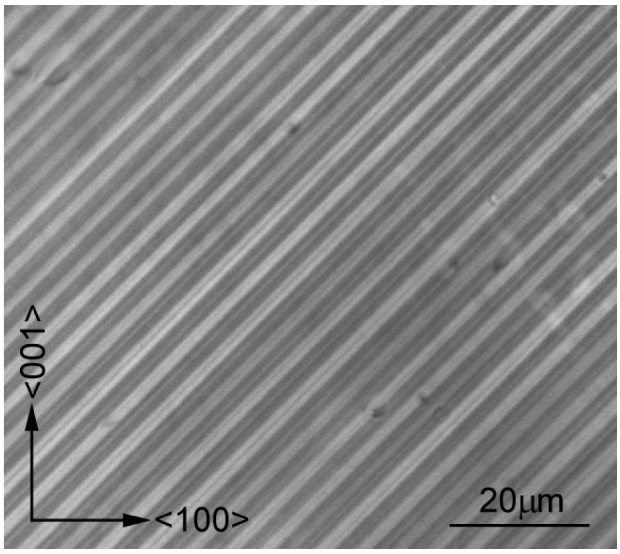

FIG. 1. Initial domain structure in the annealed specimen of 0.65PMN–0.35PT crystal.

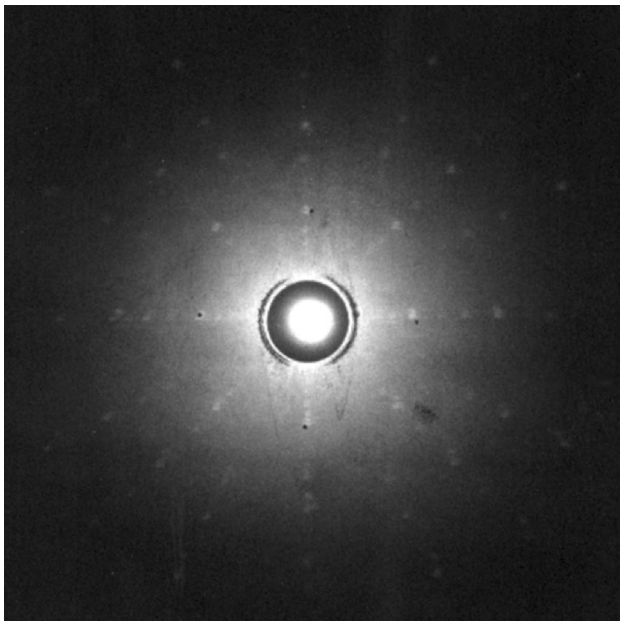

FIG. 3. X-ray Laue diffraction pattern used to determine the in-plane orientations.

III. DOMAIN INTERPENETRATION

A. Original domain structure

Optical examination indicates that the annealed crystal was occupied by several patches of regular parallel domain strips. Figure 1 shows the typical domain structure of the biggest patch, which expands over a major portion of the crystal. The annealed crystal with such domain structures was rechecked with both x-ray θ–2θ scan over $20°-50°$ and Laue diffraction. The results are shown in Figs. 2 and 3. The appearance of $(0k0)$-type peaks and the absence of other peaks in Fig. 2 confirmed that the major surface of the annealed specimen was parallel to the {010} plane. The splitting of the (002) peak from the (020) peak indicated a tetragonal structure of the crystal specimen. In addition, the much weaker intensity of the (002) peak shows that *c* domains with out-of-plane polarization occupied much less volume than *a* domains with in-plane polarization. The recheck of the annealed specimen with an x-ray Laue camera confirmed the in-plane directions, as show in Fig. 3. The in-plane ⟨100⟩ and ⟨001⟩ directions are marked in Fig. 1, and all the images shown in this article have the same orientation as Fig. 1. Based on these results, the domains shown in Fig. 1 are 90° domains with domain walls parallel to the $\{10\bar{1}\}$ plane, perpendicular to the surface. These domains are *a* domains with a ''head-to-tail'' configuration of their polarization vectors.

B. Domain interpenetration

A complex domain structure began to form after applications of a bipolar cyclic electric field to the specimen along the ⟨100⟩ direction, the horizontal direction in all images shown hence. One distinct feature of the domain structure after electrical cycling was the appearance of many domain zones, each containing parallel strips of 90° domains, as shown in Fig. 4. The domain walls in these zones are orthogonal to those of the surrounding existing domains. Ac-

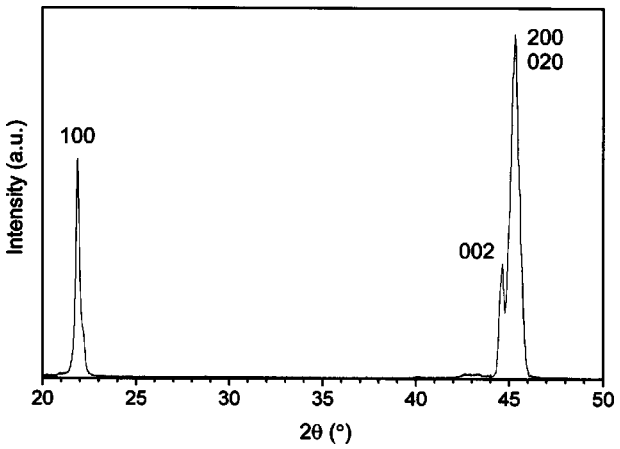

FIG. 2. X-ray diffraction indicates a {010} surface plane, a tetragonal symmetry, and a high volume fraction of *a* domains with in-plane polarization.

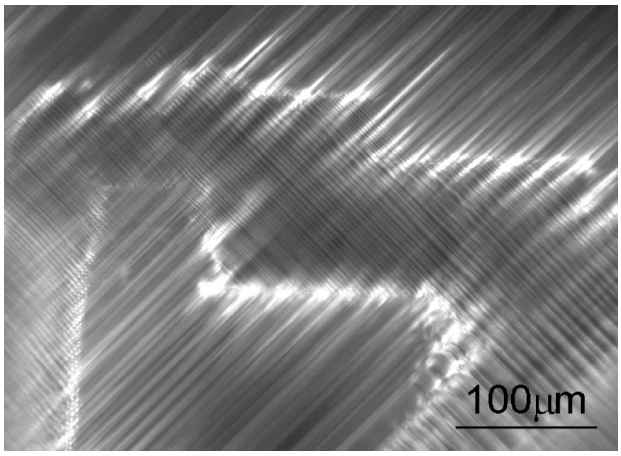

FIG. 4. Development of domain zones of 90° domain strips orthogonal to the preexisting domain strips after bipolar electric fields for 36 000 cycles at ± 4.0 kV/cm and 36 000 cycles at ± 5.0 kV/cm.

cording to their orientation and the configuration of the applied electric field, these electric field cycling-induced domains are believed to be *a* domains. The boundary between the domain zones had a bright contrast due to severe elastic distortions at domain intersections.

Closer examination of the domain structure at the zone boundary revealed the intersection of the domains [Fig. 5(a)] and interpenetration of domains [Fig. 5(b)]. For clarity, we label the thinner domains in the set of the domain strips parallel to the original strips prior to application of the external field as D_i and the thinner domains in the set of strips perpendicular to D_i as D_a.[10,17] As can be seen clearly in Fig. 5(b), domains D_a and D_i lie in the same matrix domains (the wider domains in the image, which will be denoted as D_m in Fig. 6). Analysis in the sections below will show that domains D_a and D_i have polarization vectors along the horizontal direction and domains D_m have the vector in the vertical direction. The two sets of domain strips are alternating D_i/D_m and D_a/D_m domains, respectively. In the central part of Fig. 5(a), a bright strip labeled D_i, running from the lower left to the upper right, impinges on several approaching domains. As pointed out by the bright triangles in the image, several approaching domains had full contact with the impinging domain. Simple geometrical analysis indicates that the impinging domains and the approaching domains must have antiparallel polarization directions. Therefore, the segments of the domain wall in the full contact carry electrical charges.

Next to the full contact, there was a region marked by five dark arrows in which impinging domains, D_i, had a faint contrast, making the original domain walls separate those domains less distinguishable. Instead, the impinging domains vaguely repeated dark/bright modulation of the approaching domains, suggesting that the impinging domains might have been penetrated by the approaching domains. Indeed, complete interpenetration of the approaching domains through impinging domains was found in Fig. 5(b), where the interpenetration divided the crystal into domain cells bounded on all four sides by domain walls. Behind the advancing front of the approaching domains and away from these domain cells, the original domain walls disappeared and the approaching domains replaced the original domains.

IV. DISCUSSION

Domains in ferroelectric crystals are formed to minimize depolarization energy and elastic energy. When a ferroelectric crystal contains domains of multiple polarization vectors, domains tend to assume tapered tips as they approach each other to avoid direct contact, which increases both electric and elastic energy of a ferroelectric crystal.[8,18] This study has shown that direct, full contact of domains can be produced by applying cyclic bipolar electric fields. The contact may be further extended into interpenetration of the nonparallel domain strips. Such a complex domain configuration at the intersection may be explained as follows.

Consider a tetragonal crystal that initially contains three domains, a matrix domain, D_m; an impinging domain, D_i; and an approaching domain, D_a, as shown in Fig. 6(a). The

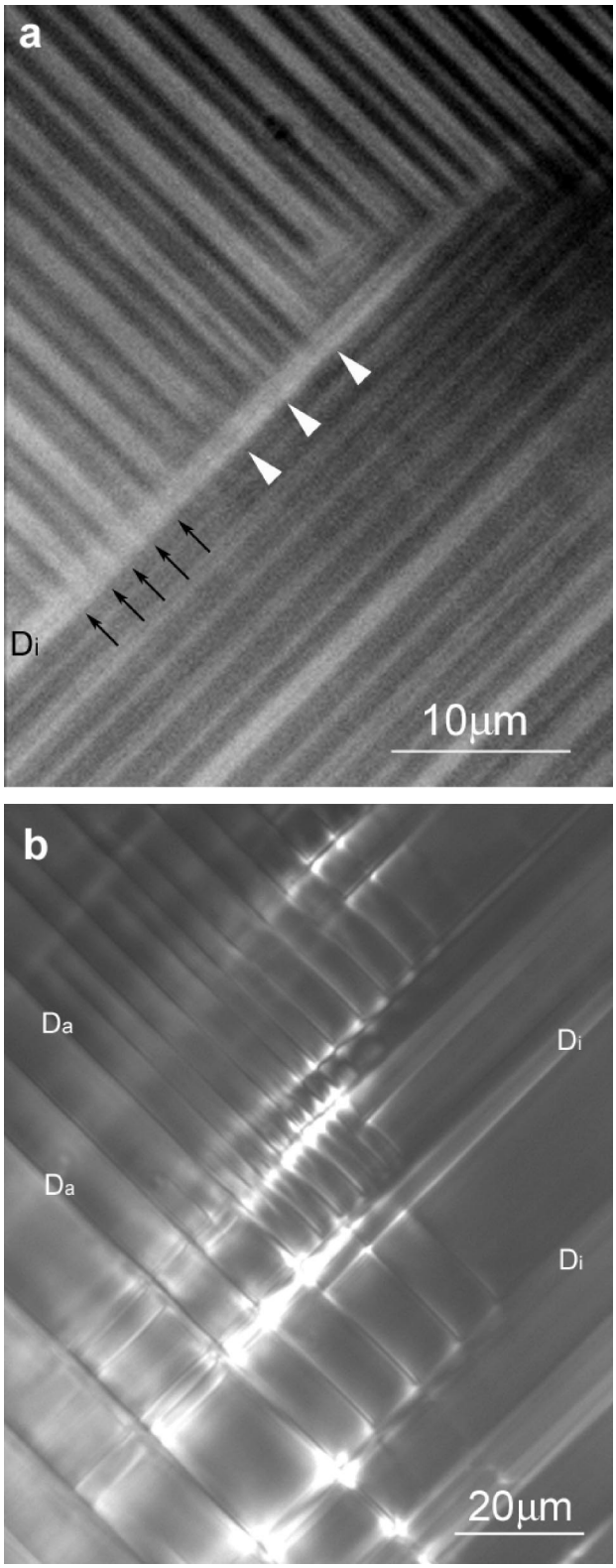

FIG. 5. Domain configurations near the zone boundary. (a) Full contact of orthogonal 90° domain strips is indicated by bright triangles. The faint contrast in the impinging domain D_i, pointed out by dark arrows, suggests the domains have grown into the D_i. (b) Interpenetration of orthogonal 90° domain strips. The approaching domains D_a penetrate the impinging domains D_i and short segments of D_i are formed.

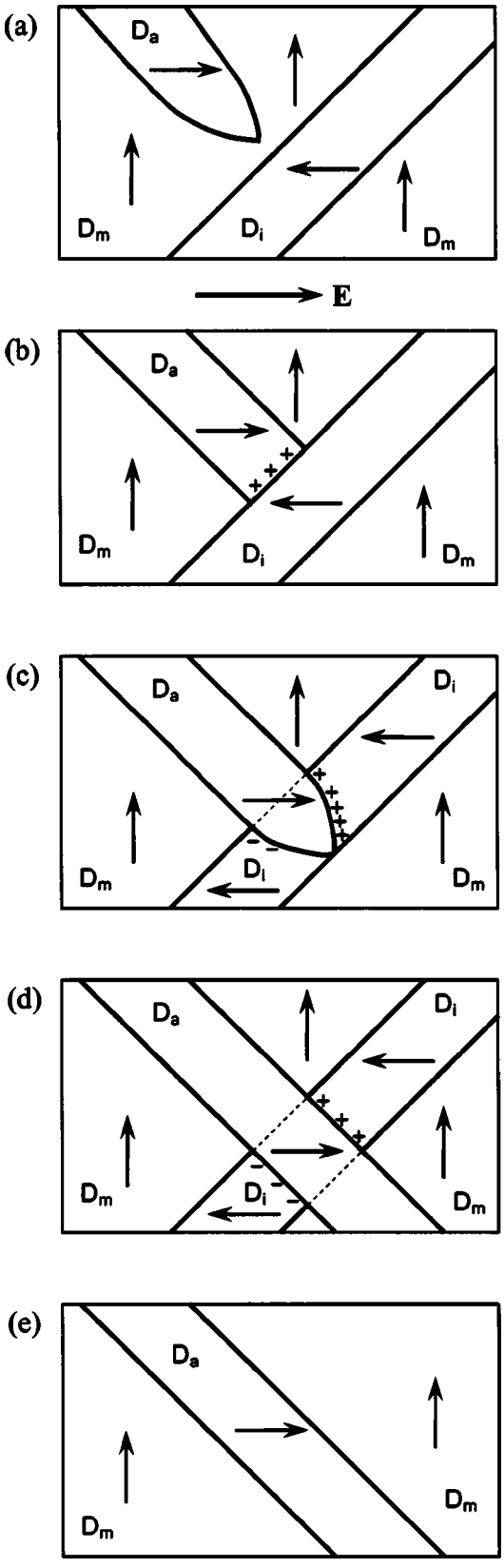

FIG. 6. Domain configurations at different stages of evolution. (a) Initial domain structure; (b) the full contact of two intersecting domains; (c) advance of the approach domain by the 180° domain switching; (d) the outgrowth step; and (e) the final withdrawal step.

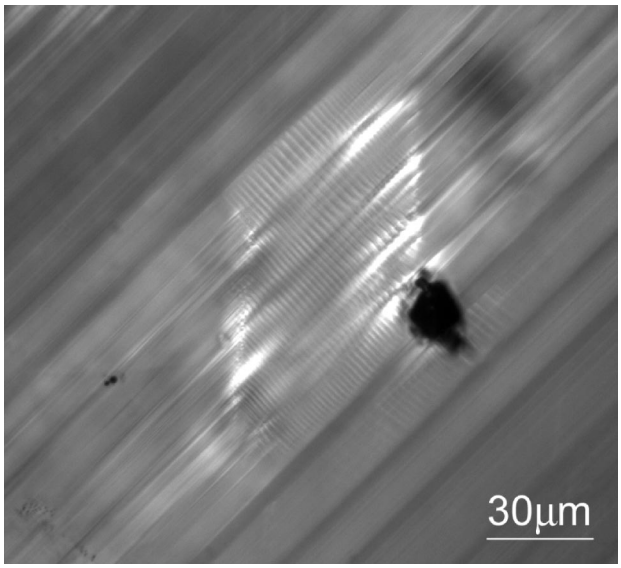

FIG. 7. Nucleation of a domain zone with orthogonal domain strips around an inclusion in an as-grown PMN–PT crystal.

matrix domain and the impinging domain represent the basic repeating units in the domain structure in Fig. 1. The approaching domain may be nucleated at a heterogeneous microstructural site such as inclusions and pores resulting from crystal growth process, microcracks generated during dicing and polishing process,[19] and the crystal/electrode interfaces.[20] As an example, Fig. 7 shows nucleation of domains around an inclusion particle in a PMN–PT crystal. In order to minimize the elastic as well as electrostatic energy, the approaching domain D_a in Fig. 6(a) assumes a tapered tip.[18] The polarizations of all three domains are shown by the arrows in Fig. 6(a). In the configuration of our tests, D_m would have a polarization vector in the vertical direction, either upward or downward. D_a and D_i should have antiparallel polarization vectors in the horizontal direction. The assignment of the polarization directions in Fig. 6(a) can be different as long as the walls are separating 90° domains with the electrically neutral ''head-to-tail'' configuration. For example, D_m could have a polarization vector pointing downward, if D_a has a polarization vector pointing to the left and D_i has a vector to the right. However, this will not change the physical picture described here. The evolution of the domain configurations at the intersection shown in Fig. 6(a) would then follow a sequence schematically depicted in Figs. 6(b)–6(e).

Under bipolar loading, the two half cycles of the applied field tend to impact these domains differently. In the positive half cycles, the field direction, denoted by the arrow between Figs. 6(a) and 6(b), is parallel to the polarization vector of D_a. For the negative half cycles, the field becomes parallel to the polarization of D_i. Therefore, the positive half cycles would facilitate the growth of the approaching domain and we will focus on this to illustrate the steps in the growth process. Similar analysis applies to the negative half cycles when the polarization vectors of the domains involved are reversed.

As D_a grows, it will be blocked by D_i. However, continued electric cycling would force D_a to make full contact with D_i even though such configuration would generate elastic distortion and electrical charge.[8,18] The result is the intersection of domains, D_a and D_i, as shown in Fig. 6(b), which agrees well with the domain configuration marked by those bright triangles in Fig. 5(a). Along the intersection, i.e., the interface between D_a and D_i (not D_m), is a 180° domain wall segment since it separates domains with antiparallel polarization vectors. However, this segment tilts away from its neutral position. For a 180° domain wall with a tilt angle θ, net electrical charges with a density of $2P \sin\theta$ are introduced at the domain wall.[18] The tilt angle for the segment in Fig. 6(b) is 45°, therefore, the charge density at this segment is $\sqrt{2}P$, where P is the polarization of the tetragonal crystal. These charges are represented by "+" in the diagram.

For the domain D_a to continue advancing, it is suggested that 180° domain switching occur in the part of the impinging domain right next to the intersection. The domain switching would result in the growth of D_a into D_i, as illustrated in Fig. 6(c). Note here that the charged wall segment in the last step disappears and two curved charged segments are formed. These two walls should be charged oppositely and contain different total charges because they have different tilting angles. D_a is expected to resume a pointed tip to minimize the elastic energy. This diagram schematically depicts the domain configuration indicated by the dark arrows in Fig. 5(a) where faint contrast was seen in the impinging domain.

The next step is the outgrowth of D_a into D_m, as illustrated in Fig. 6(d). The charges on the two wall segments between D_a and D_i (not D_m) would be redistributed. Again, these two segments would maintain opposite charges but the charge density would be the same, equal to $\sqrt{2}P$. As a result, part of the original domain walls between D_i and D_m would disappear (denoted by dotted lines) and the original long D_i would be cut into shorter segments. Between two adjacent D_a domains, cells completely enclosed by domain walls would develop, as observed in Fig. 5(b). To complete the evolution, the last step would be the withdrawal of D_i, creating a zone with domain strips orthogonal to the existing ones, as shown in Fig. 6(e). The coexistence of these domains, though in separate areas, would lead to the complex domain structure observed in Fig. 4.

V. CONCLUSIONS

Direct observations of domain structures in a tetragonal PMN–PT single crystal under cyclic bipolar electric field have shown that 90° domains with in-plane polarization vectors formed a full-contact intersection and interpentration as nonparallel sets of domain strips approached each other. While the intersection resulted in 180° domain wall segments that were electrically charged, the interpenetration of the orthogonal domains created arrays of domain cells near the boundary between two sets of the intersecting domain strips. With subsequent electric cycling, domain zones with one set of domain strips expanded at the expense of the initial domain zone. Based on experimental observations and geometric analysis, the growth of the domain zones is suggested to take four steps, namely, full contact, 180° domain switching, outgrowth, and final withdrawal/replacement.

ACKNOWLEDGMENTS

Support for this work was provided by the National Science Foundation under Grant CMS-9872306. One of the authors (X.T.) would also like to acknowledge the support from the PSI program, Ames Laboratory, U.S. Department of Energy.

[1] G. Arlt and H. Peusens, Ferroelectrics **48**, 213 (1983).
[2] S. Park and T. R. Shrout, J. Appl. Phys. **82**, 1804 (1997).
[3] S. Wada, S. Park, L. E. Cross, and T. R. Shrout, J. Korean Phys. Soc. **32**, 1290 (1998).
[4] D. Viehland, A. Amin, and J. F. Li, Appl. Phys. Lett. **79**, 1006 (2001).
[5] Y. F. Tsun and C. C. Chou, Jpn. J. Appl. Phys., Part 1 **38**, 3585 (1999).
[6] J. K. Shang and X. Tan, Acta Mater. **49**, 2993 (2001).
[7] A. Krishnan, M. E. Bisher, and M. M. J. Treacy, Mater. Res. Soc. Symp. Proc. **541**, 475 (1999).
[8] G. Arlt and P. Sasko, J. Appl. Phys. **51**, 4956 (1980).
[9] Y. H. Hu, H. M. Chan, X. W. Zhang, and M. P. Harmer, J. Am. Ceram. Soc. **69**, 594 (1986).
[10] X. Tan, J. K. Shang, and P. Han (unpublished).
[11] C. T. A. Suchicital, D. A. Payne, and A. G. de l'Eprevier, in *Proceedings of ISAF'86* (IEEE, New York, 1986), p. 465.
[12] B. M. Park and S. J. Chung, J. Am. Ceram. Soc. **77**, 3193 (1994).
[13] C. Chou, C. Chen, and D. Tseng, Mater. Chem. Phys. **45**, 103 (1996).
[14] J. Yin and W. Cao, J. Appl. Phys. **87**, 7438 (2000).
[15] J. Yin and W. Cao, J. Appl. Phys. **92**, 444 (2002).
[16] J. K. Shang and X. Tan, Acta Mater. **49**, 2993 (2001).
[17] X. Tan and J. K. Shang, Acta Mater. (submitted).
[18] A. Krishnan, M. M. J. Treacy, M. E. Bisher, P. Chandra, and P. B. Littlewood, AIP Conf. Proc. **535**, 191 (2000).
[19] Y. Hosono, K. Harada, S. Shimanuki, S. Saitoh, and Y. Yamashita, Jpn. J. Appl. Phys., Part 1 **38**, 5512 (1999).
[20] Q. Y. Jiang and L. E. Cross, J. Am. Ceram. Soc. **77**, 211 (1994).